

Is the CO Adduct of Myoglobin Bent, and Does It Matter?

THOMAS G. SPIRO*[†] AND
PAWEL M. KOZLOWSKI[‡]

*Departments of Chemistry, Princeton University,
Princeton, New Jersey 08544, and University of Louisville,
Louisville, Kentucky 40292*

Received June 5, 2000

ABSTRACT

Early reports of a severely bent CO adduct in myoglobin inspired the idea that heme proteins discriminate against CO, relative to O₂, via steric hindrance imposed by a distal histidine residue. Recent results showing that the bound CO is only slightly distorted do not by themselves overthrow the steric hypothesis, because the steric energy could be stored in displacements of the protein. However, experimental data on site-directed mutants show that the main determinant of ligand affinity changes is the polarity of the binding pocket and that H-bonding by the distal histidine accounts for about 85% of the O₂/CO discrimination while steric hindrance accounts for the remaining 15%.

Introduction

One of the more enduring controversies in chemical biology is whether nature has solved the problem of carbon monoxide toxicity by building steric hindrance into the binding pocket of the physiological oxygen carriers myoglobin and hemoglobin.^{1–8} The natural affinity of the heme prosthetic group is higher for CO than for O₂, by a factor of roughly 20 000, but this ratio is reduced to 25–200 in the proteins.⁹ The natural CO affinity is so high that we would all be asphyxiated by our own CO, which is produced naturally by catabolism of heme itself, were it not for the proteins' discrimination against CO.

The steric hindrance idea was advanced by Collman et al.¹⁰ more than 20 years ago. Noting that O₂ and CO have different geometric preferences when bound to the heme iron atom of these proteins, they hypothesized that discrimination against CO and in favor of O₂ is achieved by steric repulsion of distal residues in the protein. CO prefers to bind in an upright fashion, with linear FeCO bonding, while O₂, with two extra electrons, is naturally

Thomas G. Spiro is the Higgins Professor of Chemistry at Princeton, and former chair of the Chemistry Department. His research program focuses on the roles of metal ions in biology and the application of vibrational spectroscopy to problems in biomolecular structure and dynamics. He is also involved in research and teaching in environmental chemistry. He received the B.S. from UCLA and the Ph.D. from MIT (with David Hume) and did postdoctoral work in Copenhagen (with Carl Ballhausen) and Stockholm (with Lars Gunnar Sillén) before joining the Princeton faculty in 1963.

Pawel M. Kozlowski is Assistant Professor in the Department of Chemistry, University of Louisville. His research is concerned with the application of methods of computational chemistry to solve problems of bioinorganic structure and function. He received his M.Sc. degree from Jagiellonian University (Poland) and the Ph.D. from the University of Arizona (with Ludwik Adamowicz). He did postdoctoral work at Indiana University (with Ernest Davidson) and the University of Arkansas (with Peter Pulay). He was a research staff member of Spiro's group before he joined the University of Louisville faculty in 1999.

bent. Both myoglobin and hemoglobin have distal histidine side chains positioned over the Fe atom, which can plausibly interfere with upright binding, and thereby discriminate against CO. This attractive idea has made its way into biochemistry textbooks¹¹ (Figure 1), but it has come under increasing scrutiny and attack over the years.

This Account is an attempt to clarify this controversy. Our point of view stems from our work in vibrational spectroscopy and the vibrations of heme-bound ligands.^{12,13} Of particular relevance is the emergence of density functional theory as a method for accurately calculating vibrational spectra via the potential energy surface. The potential energy surface naturally focuses attention on energy differences among alternative ligand geometries and protein structures. Structural data alone cannot define the determinants of ligation affinities; the energetic contributions of differing structural elements, as well as contributions from the surrounding environment, must be evaluated. This observation may seem a truism, but its neglect has, in our opinion, clouded the debate over the importance of steric factors in myoglobin and hemoglobin.

MbCO Structures

Collman et al. supported their steric proposal by noting that X-ray¹⁴ and neutron¹⁵ crystal structures of the myoglobin CO adduct, MbCO, revealed a pronounced bend in the Fe–C–O angle, with reported values of 120–140°, presumably as a result of contact with the distal histidine side chain. However, these structures have engendered considerable skepticism, and the very large deviations from linearity are no longer credited. The heme binding cavity exhibited rather diffuse electron density (Figure 2), which was attributed to disorder in the CO conformation. The data were modeled with partial occupancy of alternative conformations. Ray et al.¹⁶ later analyzed the positional uncertainties of the atoms and concluded that the Fe–C–O angle must be uncertain to at least ±25°. Several other MbCO X-ray crystal structures have since been determined, which show much less apparent disorder of the CO.^{17–20} In retrospect, it seems likely that the earlier data were affected by oxidation of the protein to metMb over the course of data collection. MetMb contains Fe(III)–OH₂, and sometimes a second water molecule which is hydrogen bonded to the coordinated water.¹⁷ Thus, the electron density in the ligand pocket could reflect the partial replacement of CO by bound water. Protein stability was less an issue in the more recent determinations, which benefited from cryoscopic techniques and advances in X-ray sources and detectors, developments that have reduced collection times.

The newer crystal structures do not show the very large deviations from linearity reported earlier. Neither do crystal structures of model Fe porphyrins on which covalent superstructures have been erected in order to

[†] Princeton University.

[‡] University of Louisville.

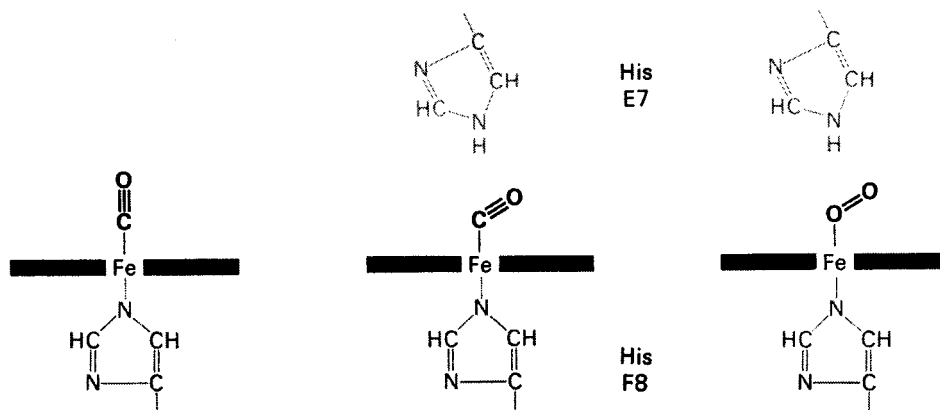


FIGURE 1. Diagram of the steric mechanism for steric inhibition of CO, but not O₂ binding (adapted from ref 11).

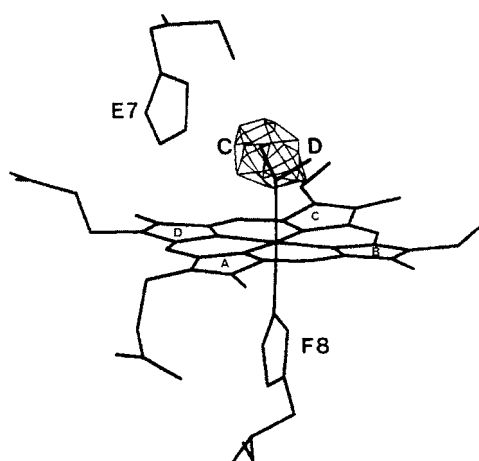


FIGURE 2. Structural diagram of the Mb binding pocket, showing the ligand electron density in the MbCO X-ray crystal structure determined by Kuriyan et al. (adapted from ref 14).

constrain the CO sterically.^{21–24} However, none of these structures have entirely upright FeCO units, and they exhibit a range of distortions. The reported results are best compared in a plot of the O atom displacement from the normal to the heme plane passing through the Fe (Figure 3), first introduced by Sage.⁶ This displacement is a result of two angular distortions, tilting and bending (see Figure 5), both of which vary from structure to structure. Even if the data from the initial X-ray and neutron structures (points 1a,b and 2a,b) are excluded from consideration, the O atom displacements range from 0.3 to 0.7 Å. The two most recent MbCO X-ray structures, obtained at very high resolution, 1.15¹⁹ and 1.20²⁰ Å, fail to narrow this range; the O atom displacements are 0.3 and 0.6 Å.

Spectroscopic data have also discounted the possibility of severe FeCO bending, but they do allow modest O atom displacements. Vibrational frequencies associated with stretching of the Fe–C and C–O bonds for a wide range of proteins and model porphyrins (having in common only the presence of a neutral imidazole sixth ligand) all fall on a single back-bonding correlation^{13,16,25} (Figure 4). The variations along this correlation are explicable on the basis of the electrostatic field in the vicinity of the bound CO,^{16,25} which polarizes the FeCO back-bonding system, driving the Fe–C and C–O frequencies in opposite directions. Deviations from this correlation are expected

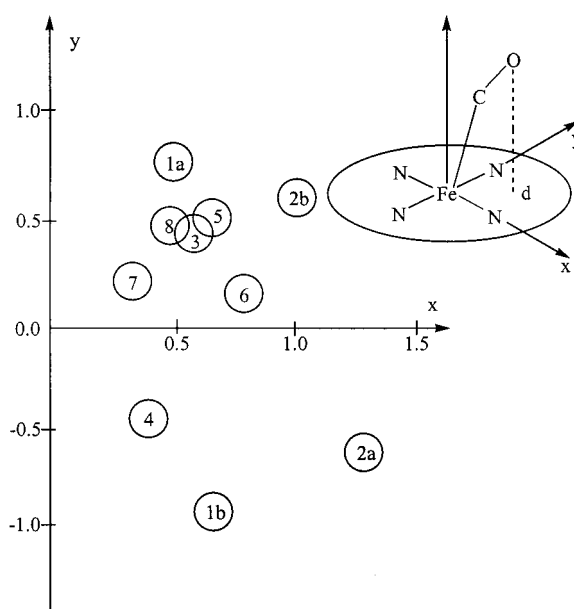


FIGURE 3. Projection of the O atom displacement from the heme z axis in MbCO crystal structures: points 1a and 1b, native $P2_1$ MbCO crystal, PDB file 1mbc, ref 14; points 2a and 2b, native $P2_1$ MbCO crystal, PDB file 2mb5, ref 15; point 3, “wild-type” D122N mutant of sperm whale myoglobin that crystallizes in a $P6$ space group, PDB file 2mgk, ref 17; points 4, 5, 6, native $P2_1$ MbCO crystals at pH 4, 5, and 6, PDB files 1spe, 1vxc, 1vxf, ref 18; point 7, $P2_1$ MbCO crystal (1.15 Å resolution), PDB file 1bzc, ref 19; point 8, $P2_1$ MbCO crystal (1.2 Å resolution), PDB file 1a6g, ref 20.

if the Fe–C–O angle is bent, because the Fe–C and C–O bonds would both weaken. Modeling of this effect via DFT¹³ calculations indicate that O atom displacements of 0.5 Å or less are consistent with the scatter of the data (Figure 4). In the same vein, variations in NMR and Mossbauer parameters can all be explained on the basis of back-bonding changes as modulated by electrostatic fields.²⁶ Again, DFT analysis of these data indicate a slightly distorted structure with tilt and bend angles of 4° and 7°.²⁷

Even smaller distortions had been indicated by IR polarization measurements on the CO stretching vibration, but reinterpretation of the results has relaxed the apparent narrowness of the constraint. The polarization can be established relative to the heme plane, either in oriented single crystals²⁸ or by photoselection of MbCO

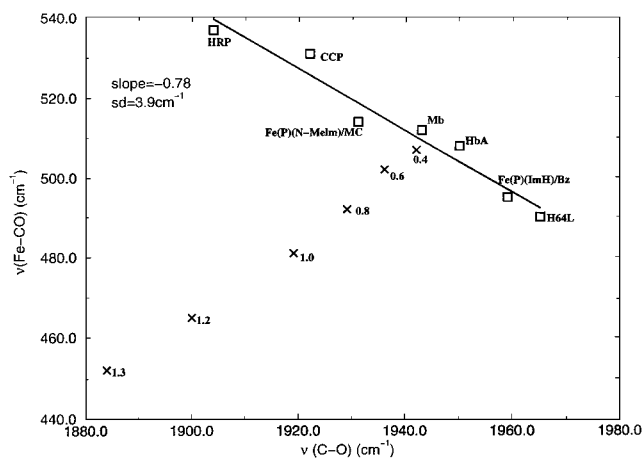


FIGURE 4. Predicted dependence of the FeCO frequencies (ν 's) on O atom displacement along the minimum energy path obtained by full vibrational calculations on structures constrained to have the indicated displacements (\AA). The squares represent experimental data for heme proteins and models.¹⁶

molecules by partial photolysis, either in frozen solution,²⁹ or by using picosecond laser pulses to freeze out protein tumbling in solution.³⁰ Photoselection measurements had earlier suggested substantial degrees of CO inclination from the heme normal, but Lim et al.,³¹ by carefully controlling the experimental variables, showed that the inclination is actually less than 7° . Meanwhile, Sage and co-workers²⁸ had determined the polarization angle in single crystals to be $6.7 \pm 0.9^\circ$, so the two techniques are in excellent agreement.

However, they both rest on the assumption that the IR polarization measures the CO bond vector. In fact, it measures the IR transition dipole direction, which is not the same thing. Although the CO oscillator is well isolated kinematically, stretching the CO bond alters the electronic distribution of the entire molecule. Because of the importance of π back-bonding from Fe to the CO, and also to the porphyrin ring, this is not a small effect. It accounts for the IR intensity, and also the frequency shift in an applied electric field (vibrational Stark effect), being much larger for heme-bound than for unbound CO.³² As the FeCO unit bends, the CO stretch sets up a dipole in the porphyrin ring which opposes that of the CO bond itself.¹³ As a result, the transition dipole inclination is less than that of the CO bond. This effect has been calculated by DFT^{13,33} and is shown in Figure 5. A 7° inclination of the transition dipole implies a 0.6 \AA displacement of the O atom, consistent with the recent crystal structures.

What then is the "real" structure of MbCO? It is not severely bent, as earlier indicated, but neither is it entirely upright. The O atom displacement is somewhere between 0.3 and 0.6 \AA , with tilt and bend angles of 5 – 10° .^{19,20} Small tilt (4°) and bend (6°) angles were also calculated by Lopez and Kollman,³⁴ using molecular dynamics on the MbCO structure. (In their abstract, Lopez and Kollman reported a more distorted structure, with 20° of bend and 6° of tilt, but this was based on a calculation with the N δ H tautomer of the distal histidine, the tautomer reported from neutron crystallography.¹⁵ Calculations with the N ϵ H tautomer,

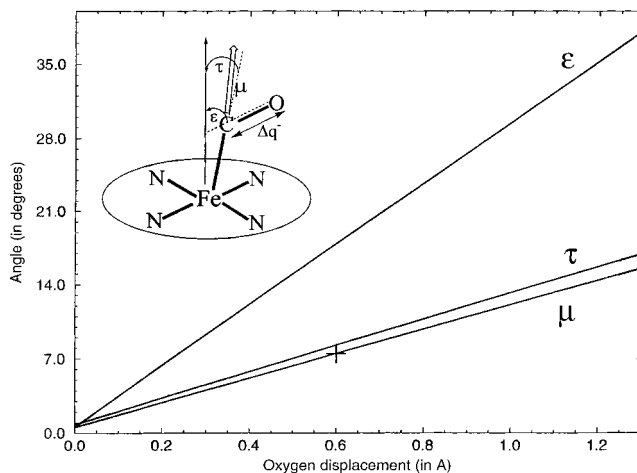


FIGURE 5. Calculated CO stretching transition dipole direction (μ) along the DFT minimum energy distortion path.³³

which is almost certainly the correct tautomer for the CO adduct—see below—gave the less distorted structure.)

Bending Energy

Does the downward revision of the extent of FeCO distortion in MbCO disqualify the steric hindrance proposal of Collman et al.? It does not. The steric hindrance could equally well be accommodated by displacements of the protein itself. The study of superstructured porphyrins has made it clear that steric forces can strongly discriminate between CO and O₂,^{2,8,23} yet crystal structures of the CO adduct show only small FeCO distortions.^{8,21–24} There are, however, large displacements of the superstructure, together with distortion of the porphyrin ring. Ironically, the original reports of large FeCO distortions in MbCO ultimately obscured the steric hindrance hypothesis by focusing too much attention on this structural anomaly.

How much steric energy do the newer, less-distorted MbCO structures imply? Until recently, the FeCO bonds had been thought to be quite stiff, because the vibrational frequency of the Fe–C–O bending mode, $\sim 570 \text{ cm}^{-1}$, is high, higher than the frequency of the Fe–C stretching mode ($\sim 500 \text{ cm}^{-1}$).³⁵ However, Ghosh and Bocian^{4,36} discovered via a DFT analysis of the vibrations that the elevated bending frequency results from a large positive interaction force constant between the bending and tilting coordinates, and that the energy required to distort the FeCO unit is actually quite modest. We confirmed this result at a higher level of DFT² and calculated the energy as a function of the O atom displacement by constraining only this parameter, for an imidazole–(Fe^{II} porphyrin)–CO model, and allowing all other structural parameters to relax to the minimum energy geometry.¹³ The resulting minimum energy distortion curve (Figure 6) is much lower than the curves calculated if the distortion were limited to only bending or only tilting. The range of distortions derived from the more recent structures requires small amounts of energy, 0.3 – 1.1 kcal/mol for 0.3 – 0.6 \AA displacements of the O atom.¹³

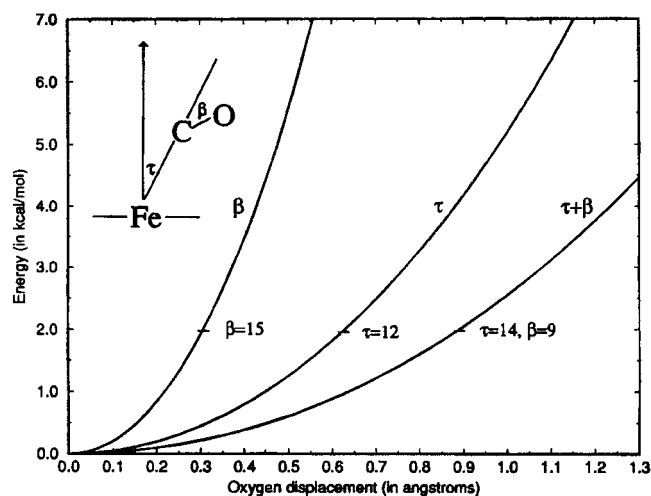


FIGURE 6. Energy for displacement of the O atom from the heme normal calculated via DFT for bending (β), tilting alone (τ), and a minimum energy combination of bending and tilting.¹³

The steric energy stored in protein displacements is harder to evaluate. Long ago, Case and Karplus³⁷ estimated 7 kcal/mol as the upper bound on the energy that the protein could exert on the CO ligand, via a molecular mechanics calculation of side-chain reorientations on a rigid backbone. More recently, Lopez and Kollman³⁴ used free energy perturbation methods to calculate the van der Waals energy contribution to the discrimination between CO and O₂, and they concluded that it is only on the order of 0.5 kcal/mol. However, evaluating the energies of the many small displacements which are evident in the crystal structures puts severe demands on the available force fields.

Elsewhere we have assumed that the protein stores as much energy as the FeCO distortion energy, and that doubling the distortion energy gives a reasonable estimate of the total steric energy, i.e., 0.6–2.2 kcal/mol for 0.3–0.6 Å O atom displacements. However, the energy need not be equally partitioned (the forces on interacting atoms must be equal and opposite, but the associated energies need not be equal), and it is possible that the protein stores “excess” steric energy. This possibility is illustrated by the superstructured porphyrins. For example, the CO affinity of the 1,2-dimethylimidazole adduct of Fe^{II}-PocPiv,²¹ a derivative of “picket-fence” porphyrin in which a capping benzene ring is attached to three of the pivaloylamido pickets by methylene bridges, is 2.5 kcal/mol smaller than it is for Fe^{II}Piv₃5Cim, another picket-fence porphyrin derivative which lacks the benzene cap, but in which one of the pickets is attached to an internally coordinated imidazole.³⁸ The electronic environments of these two porphyrins are very similar, so that the affinity lowering is attributable to the steric hindrance of the cap. The crystal structure of the CO adduct shows a small FeCO distortion, with a 0.4 Å O atom displacement, corresponding to an FeCO distortion energy of 0.5 kcal/mol, on the basis of the DFT curve. This is only 20% of the 2.5 kcal/mol total steric energy. The remainder must be provided

by the substantial distortions in the porphyrin and its superstructure.²¹

Could the residue displacements observed in MbCO relative to those in deoxyMb^{14–20} carry significant steric energy? We return to this question after first considering electrostatic effects.

Electrostatics and H-Bonding

The alternative to the steric hypothesis is that discrimination in favor of O₂ results from a stabilizing H-bond interaction with the distal histidine. This idea can be traced back to a suggestion of Pauling in 1964^{39a} and has been supported by model studies from the 1980s onward which demonstrated an important influence of polarity on the binding of O₂, but not CO, to the heme group. (For reviews, see refs 8 and 23). An H-bond between the distal histidine and bound O₂ has been clearly identified by neutron diffraction^{39b} and NMR,^{39c} and a weak H-bond to bound CO is suggested by D₂O sensitivity of the FeCO vibrations.^{39d} Both ligands rely on back-donation of electrons from the heme Fe(II), but the transfer of charge is much greater for O₂ than for CO. Consequently, polar interactions with distal residues carry more energy for O₂ than for CO.

This differential effect has been extensively investigated in myoglobin by Olson, Phillips, Sligar, Springer, Wilkinson, Ikeda-Saito, and co-workers, using site-directed mutagenesis.⁹ Altering the polarity of residues in the binding pocket produces major changes in the affinity and dissociation rate for O₂ but minor ones for CO. Paradoxically, it is the CO adduct that provides a convenient measure of the pocket polarity,^{9,32} because of the accessibility of the CO and FeC stretching frequencies in the IR and Raman spectra and the ¹³C chemical shift in the NMR spectrum. All of these respond sensitively to polarity changes because of the resulting shift in the extent of back-bonding. However, the energy differences are small, and the CO dissociation rates correlate only weakly with these spectral parameters.⁹

The O₂ dissociation rates, on the other hand, correlate strongly with the CO spectral parameters. Phillips et al.⁴⁰ have recently shown that this correlation can be attributed quantitatively to the pocket polarity. For both ligands, the log of the dissociation rate correlates linearly with the electrostatic potential at the ligand atoms, calculated via a linearized Poisson–Boltzmann method for a series of mutant myoglobin crystal structures. However, the slope of the correlation is 4 times larger for O₂ than for CO (Figure 7). Since the log of the dissociation rate is expected to be directly related to the bond strength, the electrostatic correlations imply that a given polar influence, e.g., an H-bond, carries 4 times more energy for O₂ than for CO. Encouragingly, the H-bond energy calculated via DFT by Sigfridsson and Ryde⁴¹ for imidazole interacting with a ligated heme was also 4 times greater for O₂ than for CO. The absolute energies, 7.6 and 1.9 kcal/mol, respectively, were recognized by the authors to be too high, but the ratio is in agreement with the experimental results of Phillips et al. on myoglobin. Using free energy perturba-

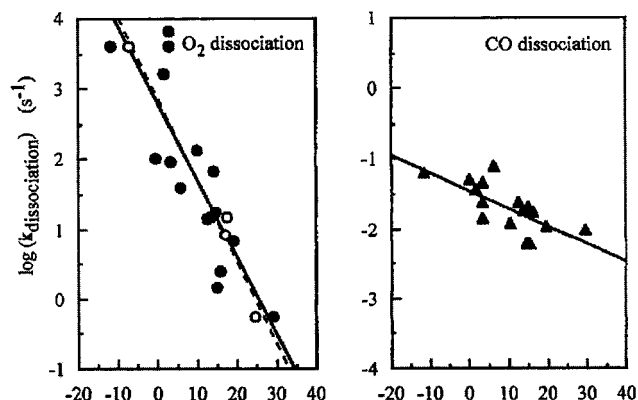


FIGURE 7. Correlations of O₂ and CO dissociation rate constants with the electrostatic potential at the O atom (units in kcal/mol) calculated using MbO₂ (open circles) or MbCO (filled symbols) crystal structures (adapted from ref 40).

tion methods and the AMBER empirical force field,⁴² Lopez and Kollman³⁴ calculated 1.9 kcal/mol as the difference in the histidine–ligand electrostatic energy between O₂ and CO for the N–H tautomer; curiously, however, almost the same difference, 1.7 kcal/mol, was calculated when MbCO had the N–H tautomer.

The correlation of the CO stretching frequency with the calculated electrostatic potential only works if the NεH tautomer is assumed, i.e., with the NH group pointing at the CO; the correlation is poor if the NδH tautomer is assumed.⁴⁰ Although neutron crystallography gives a clear-cut location for the imidazole proton,¹⁵ Phillips et al.⁴⁰ point out that the NδH tautomer could well have been produced by the same autoxidation to metMb that likely produced the apparent FeCO distortion, since replacement of Fe^{II}CO by Fe^{III}H₂O could reverse the H-bonding with the distal histidine.⁴³ Interestingly, binding of NO to Fe^{III}Mb also appears to favor the NδH tautomer; the NO stretching frequency is 20 cm⁻¹ lower than it is in the H64L mutant, suggesting a negative polar interaction with the N⁻ lone pair.⁴⁴ Although Fe^{III}NO⁺ is isoelectronic with Fe^{II}-CO, the positive charge apparently induces a tautomeric shift in the distal histidine.

Quantitative Evaluation of Energy Contributions from Mutants

Olson and Phillips⁷ have argued that the electrostatic mechanism is mainly responsible for the ~1000-fold reduction in the ratio of the CO and O₂ affinity constants in Mb, and that steric hindrance is less important. The main evidence is the ~500-fold increase in the O₂ dissociation rate constant when the distal histidine in myoglobin is replaced with a hydrophobic residue. To be sure, the CO affinity increases, but only by a factor of ~10, and this factor can be attributed to the displacement of a water molecule which is H-bonded to the distal histidine in the deoxy form of the protein, and which is not present in the hydrophobic mutants. Thus, there appears to be little room for a steric influence by the distal histidine.

The steric vs electronic issue can be approached quantitatively with the aid of the full set of kinetic and

equilibrium constants determined by Olson and co-workers. We can estimate the various binding energy contributions in the following way.

The change in the ligand binding free energy for a residue substitution in myoglobin is obtained via

$$kT\Delta \ln K_L = \Delta\Delta G_L \quad (1)$$

where K_L is the equilibrium constant for the reaction Mb + L = MbL. We decompose this change into three terms

$$\Delta\Delta G_L = \Delta E_L - \Delta St_L - \Delta E_{dx} \quad (2)$$

ΔE_L is the change in the electrostatic stabilization energy from the field in the binding pocket, while ΔSt_L is the change in the steric interaction energy that opposes ligand binding. ΔE_{dx} is an energy term for deoxyMb, whose main contribution is from the water molecule which is H-bonded to the distal histidine in the wild-type protein. This term is the same whether CO or O₂ is the ligand.

We assume that for O₂ steric hindrance is absent and $\Delta St_{O_2} = 0$. Then, ΔE_{dx} and ΔSt_{CO} can be obtained from the experimental values of $\Delta\Delta G_L$ for CO and O₂, if the electrostatic energies, ΔE_L , can be estimated independently.

To do this, we turn to the dissociation rate constants, k_L , and assume that the activation energy for ligand dissociation is just the bond dissociation energy, which is the sum of the intrinsic bond energy, D_L , and the electrostatic stabilization energy imposed by the protein,

$$E_a = D_L + E_L \quad (3)$$

where $k_L = Ae^{E_a/kT}$. This assumption ignores protein effects on the nascent products, namely the deoxy-heme and the dissociated but protein-localized ligand molecule. These effects on the activation energy may not be negligible (see below, in connection with the leucine mutant) but are likely to be small compared to the electrostatic interaction with the bound ligand. Since D_L is independent of the protein, the effect of a residue substitution on the electrostatic stabilization is obtained from

$$\Delta E_L = kT\Delta \ln k_L \quad (4)$$

(We note that ΔE_L includes changes in bond strength which are induced by the electric field of the protein, as reflected in the changes observed for the Fe–L stretching frequency.¹⁶) In Table 1, we list measured values for k_L and K_L for wild-type myoglobin, both sperm whale and human, and for three mutants, in which the distal histidine (residue E7) is replaced by valine, isoleucine, and leucine, hydrophobic amino acids having isopropyl, *sec*-butyl and *isobutyl* side chains. These were selected from among the many mutants studied by Olson and co-workers because the side chains are hydrocarbons of about the right size to replace the histidine side chain. Larger ones (e.g., Phe and Trp) may exert extra steric force, while smaller ones (e.g., Gly and Ala) may leave room for water in the ligated protein, something that has been

Table 1. O₂ and CO Dissociation Rate Constants (*k*, s⁻¹) and Binding Constants (*K*, μM⁻¹) (from Ref 40) for Myoglobin Variants, and Calculated Interaction Energies (kcal/mol)^a

variant	<i>k</i> _{O₂}	Δ <i>E</i> _{O₂}	<i>k</i> _{CO}	Δ <i>E</i> _{CO}	<i>K</i> _{O₂}	ΔΔ <i>G</i> _{O₂}	Δ <i>E</i> _{dx}	<i>K</i> _{CO}	ΔΔ <i>G</i> _{CO}	Δ <i>St</i> _{CO}	ΔΔΔ <i>G</i> _{CO-O₂}
sperm											
E7His	15		0.019		1.1			27			
E7Val	10 000	3.84	0.048	0.55	0.011	-2.72	1.12	150	1.01	0.44	3.73
E7Ile	6 400	3.58	0.047	0.54	0.014	-2.46	1.12	170	1.09	0.50	3.55
E7Leu	4 100	3.31	0.024	0.14	0.023	-1.68	1.08	1100	2.19	1.25	3.87
human											
E7His	22		0.022		0.86			35			
E7Val	7 700	3.46	0.051	0.50	0.011	-2.58	0.88	100	0.62	0.24	3.20
E7Ile	11 000	3.67	0.044	0.41	0.0072	-2.82	0.85	130	0.78	0.33	3.60
E7Leu	5 400	3.35	0.029	0.16	0.022	-2.16	1.08	880	1.90	0.98	4.06
average		3.5		0.4			1.0			0.6	3.7
(less E7Leu)		3.6		0.5			1.0			0.4	3.5

^a Symbols: Δ*E*_L = *kT*Δ ln *k*_L; ΔΔ*G*_L = *kT*Δ ln *K*_L, where Δ is the difference between wild-type Mb (E7His) and the indicated mutant. Δ*E*_{dx} = Δ*E*_{O₂} - ΔΔ*G*_{O₂}; Δ*St*_{CO} = Δ*E*_{CO} - Δ*E*_{dx} - ΔΔ*G*_{CO}; ΔΔΔ*G*_{O₂-CO} = ΔΔ*G*_{O₂} - ΔΔ*G*_{CO}.

observed in the E7Gly crystal structure.⁹ Also listed are values of Δ*E*_L, Δ*E*_{dx}, and Δ*St*_{CO}, calculated via eqs 1, 2, and 4.

For O₂, the three hydrophobic E7 residue replacements increase *k*_L by a factor of 385, on average, giving 3.5 kcal/mol for Δ*E*_{O₂}. For CO, *k*_L also increases but by a much smaller factor, 1.9 on average, giving 0.4 kcal/mol for Δ*E*_{CO}. The results are consistent for myoglobin from sperm whale and from humans. We identify the Δ*E*_L's with the strength of the H-bond interaction between the distal histidine and the bound O₂ and CO ligands. Encouragingly, the value for CO agrees well with the 0.5 kcal/mol estimate made earlier¹⁶ from the correlation of the CO infrared frequency with *k*_L values. The ratio of H-bond strengths for O₂ and CO is higher than the value of 4 which was estimated above from the dependence of *k*_L on the calculated electric potential,⁴⁰ or from the DFT model results,⁴¹ but this could reflect a less-than-optimal alignment of the histidine side chain with respect to the bound CO. Precisely because the bound O₂ and CO have different geometries, their interaction with specific residues will differ somewhat. Indeed, Phillips et al.⁴⁰ found that the correlation of *k*_L vs electrostatic potential for O₂ improved if structural data for the O₂ adducts were substituted for those of the CO adducts (see Figure 7).

The six entries in Table 1 for Δ*E*_{dx} give an average value of 1.0 kcal/mol for the H-bond between the distal histidine and the water molecule in the deoxyMb structure. This is a low H-bond value but is consistent with several lines of evidence cited by Olson and Phillips⁷ that the occupancy factor for this water molecule is only about 90%. The six values for Δ*St*_{CO} average to 0.6 kcal/mol. Thus the steric inhibition to CO binding by the distal histidine does indeed appear to be very modest, and accounts for a minor part of the discrimination energy.

The discrimination energy is the difference between ΔΔ*G*_L values for CO and O₂ (last column of Table 1). We obtain an average value of 3.7 kcal/mol as a measure of the contribution of the histidine residue to the ligand discrimination. (This is twice the value calculated by Lopez and Kollman³⁴ using free energy perturbation and the AMBER force field⁴²). This value is sufficient to account for the entire ligand discrimination effect of Mb relative to protein-free heme. Thus, the distal histidine is, indeed,

the key residue in adjusting the relative ligand affinities. The 3.7 kcal/mol of discrimination energy is made up of a 0.6 kcal/mol steric contribution and a 3.1 kcal/mol electrostatic contribution, the difference between the H-bond energies for bound O₂ and CO. On the basis of these estimates, the steric contribution accounts for about one-sixth of the discrimination, the remainder being due to the stronger H-bond to O₂ than to CO.

The individual entries in Table 1 show some dispersion, as expected from the simplified nature of the model we employ. Each mutation creates numerous small changes in the inter-residue interactions. The leucine mutant is an outlier, whose anomalous character has been noted by Phillips and Olson.⁷ The main anomaly is the very high value of *K*_{CO}, ~1000 μM⁻¹, vs ~150 μM⁻¹ for the valine and isoleucine mutants. Likewise, *K*_{O₂} is higher for leucine, although the elevation is not as dramatic. In addition, *k*_L is barely altered for CO, relative to that for the wild-type protein, resulting in an anomalously low Δ*E*_{CO}. The value of Δ*E*_{O₂} is also depressed, relative to the values for the other mutants. This pattern of anomalies is the same for the sperm whale and human mutants. We speculate that the leucine side chain provides a particularly favorable environment for the nascently dissociated ligand, which is known to be located in a pocket next to the heme.^{5,45,46} This stabilization can explain the increase in fraction of geminate CO recombination which is observed immediately after photolysis of the CO adduct of the Leu64 mutant.^{47,48} An increase in internal rebinding increases the overall association rate constant and lowers the dissociation rate constant, producing a lower apparent Δ*E*_L value. This extra stabilization could also account for a higher ligand affinity because the free energies for forming the heme-bound and protein-bound ligand states are additive.

If the leucine mutant is excluded from the averages, then the energy estimates change only slightly. Δ*E*_L increases by 0.1 kcal/mol, for both ligands, leaving the electrostatic contribution to the discrimination at 3.1 kcal/mol. Δ*E*_{dx} is unaltered, while Δ*St*_{CO} diminishes, from 0.6 to 0.4 kcal/mol, thus accounting for one-ninth of the total discrimination energy.

These estimates of Δ*St*_{CO}, 0.6 or 0.4 kcal/mol, are at the low end of the range of estimates based on the DFT-computed distortion energies, implying that, unlike the

superstructured porphyrin model compounds, the distal histidine stores very little excess steric energy. This is not entirely surprising since the crystal structures show the E7 imidazole side chain to be rather flexible, as indicated by high-temperature factors¹⁹ or significant population of alternative orientations.²⁰

Recently, Kachalova et al.¹⁹ have proposed a different steric mechanism that could potentially carry excess energy, like the model compounds. Analysis of their high-resolution structures revealed a ligation-induced concerted motion of the distal (F) and proximal (E) helices, which hold the heme like a clamshell. (Elsewhere we have proposed that a similar concerted motion is the first step in the allosteric transition of hemoglobin⁴⁹). They noted, that unlike histidine E7, another contacting residue, valine E11, is well-packed in the pocket but is displaced 0.5 Å between MbCO and deoxyMb, and they proposed that this displacement is linked to the concerted helix movements.

Replacement of valine E11 with the smaller alanine residue (which has no effect on the CO dissociation rate, as expected) does selectively increase the CO binding constant, but only by a factor of 2,⁹ showing that the contribution to ligand discrimination by the steric hindrance of valine E11 is worth only 0.4 kcal/mol. Substitution of E11 by the larger isoleucine residue⁹ inhibits CO binding by a much larger factor, ~13, showing that steric hindrance at this position is certainly possible. However, the affinity of myoglobin for O₂ is also reduced significantly, ~6-fold, by the Ile68 substitution. Thus, although there is selective steric discrimination against CO binding, the effect is again only a factor of ~2.

Summary

Early reports that the FeCO unit is severely bent in MbCO are generally agreed to have been incorrect. All recent experimental data point to a small and somewhat variable distortion, with the O atom displaced from the heme normal by 0.3–0.6 Å. The energy required for this extent of distortion is quite small, because of interaction between bending and tilting coordinates. DFT computation yields 0.3–1.1 kcal/mol. However, these facts are not in themselves sufficient to overthrow the steric mechanism for ligand discrimination, because they do not address the amount of steric energy stored by the protein. The finding that FeCO is only slightly distorted in sterically encumbered model compounds with significantly diminished CO affinity underscores the possibility that the protein could, in principle, store significant steric energy.

Nevertheless, the results of site-directed mutagenesis establish fairly clearly that this does not happen. Analysis of the kinetic and equilibrium data indicates that the steric inhibition of CO binding is worth about 0.5 kcal/mol. The rest of the ca. 3.5 kcal/mol of discrimination in favor of O₂ is attributable to H-bonding by the distal histidine side chain, which is much stronger to bound O₂ than to bound CO.

There are two important differences in the properties of heme-bound CO vs O₂. The first is the geometry

difference: FeO₂ is naturally bent, while FeCO is linear. The second is the polarity difference: more negative charge is transferred to the ligand in FeO₂ than in FeCO. Both offer a potential mechanism for ligand discrimination. Nature has mainly exploited the polarity difference in achieving discrimination. One can speculate that it is easier to place H-bond donors at strategic positions in the protein than it is to engineer a protein scaffold near the iron atom that is rigid enough to exploit small geometry differences between the bound ligands.

We thank Prof. John Olson for insightful comments and helpful suggestions during the preparation of this Account, and we gratefully acknowledge the contributions of our collaborators, whose names are listed in appropriate references, especially Dr. Marek Zgierski, who has been closely involved in our DFT computations.

References

- (1) For a recent news account, see: Borman, S. A Mechanism Essential to Life. *Chem. Eng. News* **1999**, Dec 6, 31–36.
- (2) Spiro, T. G.; Kozlowski, P. M. Will the Real FeCO Please Stand up? *J. Biol. Inorg. Chem.* **1997**, *2*, 516–520.
- (3) Slebodnick, C.; Ibers, J. A. Myoglobin Models and Steric Origins of the Discrimination Between O₂ and CO. *J. Biol. Inorg. Chem.* **1997**, *2*, 521–525.
- (4) Vangberg, T.; Bocian, D. F.; Ghosh, A. Deformability of Fe(II)CO and Fe(III)CN Groups in Heme Protein Models: Nonlocal Density Functional Theory Calculations. *J. Biol. Inorg. Chem.* **1997**, *2*, 526–530.
- (5) Lim, M.; Jacson, T. A.; Anfinsenrud, P. A. Modulating Carbon Monoxide Binding Affinity and Kinetics in Myoglobin: the Roles of the Distal Histidine and the Heme Pocket Docking Site. *J. Biol. Inorg. Chem.* **1997**, *2*, 531–536.
- (6) Sage, T. J. Myoglobin and CO: Structure, Energetics, and Disorder. *J. Biol. Inorg. Chem.* **1997**, *2*, 537–543.
- (7) Olson, J. S.; Phillips, G. N. Myoglobin Discriminates Between O₂, NO, and CO by Electrostatic Interactions with the Bound Ligand. *J. Biol. Inorg. Chem.* **1997**, *2*, 544–552.
- (8) Collman, J. P.; Fu, L. Synthetic Models for Hemoglobin and Myoglobin. *Acc. Chem. Res.* **1999**, *32*, 455–463.
- (9) Springer, B. A.; Sligar, S. G.; Olson, J. S.; Phillips, G. N., Jr. Mechanisms of Ligand Recognition in Myoglobin. *Chem. Rev.* **1994**, *94*, 699–714.
- (10) Collman, J. P.; Brauman, J. I.; Halbert, T. R.; Suslick, K. S. Nature of O₂ and CO Binding to Metalloporphyrins and Heme Proteins. *Proc. Natl. Acad. Sci. U.S.A.* **1976**, *73*, 3333–3337.
- (11) Stryer L. *Biochemistry*, 3rd ed.; Freeman: New York, 1988; p 149.
- (12) Spiro, T. G.; Zgierski, M. Z.; Kozlowski, P. M. Stereoelectronic Factors in CO, NO and O₂ Binding to Heme From Vibrational Spectroscopy and DFT Analysis. *Coord. Chem. Rev.*, submitted.
- (13) Kozlowski, P. M.; Vogel, K. M.; Zgierski, M. Z.; Spiro, T. G. Steric Contributions to CO Binding in Heme Proteins: A Density Functional Analysis of FeCO Vibrations and Deformability. *J. Porph. Phthal.* **2000**, in press.
- (14) Kuriyan, J.; Wilz, S.; Karplus, M.; Petsko, G. A. X-ray Structure and Refinement of Carbon-monooxy Fe(II)-myoglobin at 1.5 Å Resolution. *J. Mol. Biol.* **1986**, *192*, 133–154.
- (15) Cheng, X.; Schoenborn B. *Acta Crystallogr.* **1990**, *B46*, 195. Cheng X.; Schoenborn B. Neutron Diffraction Study of Carbon Monooxy-myoglobin. *J. Mol. Biol.* **1991**, *220*, 381–399. Norvell, J. C.; Nunes, A. C.; Schoenborn, B. P. *Science* **1975**, *190*, 568. Hanson, J. C.; Schoenborn, B. P. *J. Mol. Biol.* **1981**, *153*, 117.
- (16) Ray, G. B.; Li, X.-Y.; Ibers, J. A.; Sessler, J. L.; Spiro T. G. How Far Can Proteins Bend the FeCO Unit? Distal Polar and Steric Effects in Heme Proteins and Models. *J. Am. Chem. Soc.* **1994**, *116*, 162–176.
- (17) Quillin, M. L.; Arduini, R. M.; Olson, J. S.; Phillips, G. N., Jr. High-Resolution Crystal Structures of Distal Histidine Mutants of Sperm Whale Myoglobin. *J. Mol. Biol.* **1993**, *234*, 140–155.
- (18) Young F.; Phillips G. N., Jr. Crystal structures of CO-, deoxy- and met-myoglobins at various pH values. *J. Mol. Biol.* **1996**, *256*, 762.
- (19) Kachalova, G. S.; Popov, A. N.; Bartunik, H. D. A Steric Mechanism for Inhibition of CO Binding to Heme Proteins. *Science* **1999**, *284*, 473–476.

- (20) Vojtechovsky, J.; Chu, K.; Berendzen, J.; Sweet, R. M.; Schlichting, I. Crystal structures of myoglobin-ligand complexes at near-atomic resolution. *Biophys. J.* **1999**, *77*, 2153.
- (21) Kim, K.; Fettinger, J.; Sessler, J. L.; Cyr, M.; Hugdahl, J.; Coleman, J. P.; Ibers, J. A. Structural Characterization of a Sterically Encumbered Iron(III) Porphyrin CO Complex. *J. Am. Chem. Soc.* **1989**, *111*, 403.
- (22) Kim, K.; Ibers, J. Structure of a carbon-monoxide adduct of a capped porphyrin-Fe(C2-CAP)(CO)(1-Methylimidazole). *J. Am. Chem. Soc.* **1991**, *113*, 6077.
- (23) Momenteau, M.; Reed, C. A. Synthetic Heme Dioxxygen Complexes. *Chem. Rev.* **1994**, *94*, 659–698.
- (24) Slebodnick, C. J.; Fettinger, C.; Peterson, H. B.; Ibers, J. A. Structural characterization of five sterically protected porphyrins. *J. Am. Chem. Soc.* **1996**, *118*, 3216.
- (25) Li, X.-Y.; Spiro, T. G. Is Bound CO Linear or Bent in Heme-Proteins—Evidence from Resonance Raman and Infrared Spectroscopic Data. *J. Am. Chem. Soc.* **1988**, *110*, 6024.
- (26) Godbout, N.; Havlin, R.; Salzman, R.; Debrunner, P. G.; Oldfield, E., Iron-57 NMR Chemical Shifts and Mossbauer Quadrupole Splittings in Metalloporphyrins, Ferrocyclochrome *c*, and Myoglobins: A Density Functional Theory Investigation. *J. Phys. Chem. A* **1998**, *102*, 2342.
- (27) McMahon, M. T.; de Dios, A. C.; Godbout, N.; Salzman, R.; Laws, D. D.; Le, H.; Havlin, R. H.; Oldfield, E. An Experimental and Quantum Chemical Investigation of CO Binding to Heme Proteins and Model Systems: A Unified Model Based on ¹³C, ¹⁷O, and ⁵⁷Fe Nuclear Magnetic Resonance and ⁵⁷Fe Mossbauer and Infrared Spectroscopies. *J. Am. Chem. Soc.* **1998**, *120*, 4784–4797.
- (28) Ivanov, D.; Sage, J. T.; Keim, M.; Powell, J. R.; Asher, S. A.; Champion, P. M. Determination of CO Orientation in Myoglobin by Single-Crystal Infrared Linear Dichroism. *J. Am. Chem. Soc.* **1994**, *116*, 4139–4140. Sage, J. T. Infrared Crystallography: Structural Refinement Through Spectroscopy. *Appl. Spectrosc.* **1997**, *51*, 568. Sage, J. T.; Jee, W. *J. Mol. Biol.* **1997**, *274*, 21.
- (29) Ormos, P.; Braunstein, D.; Frauenfelder, H.; Hong, M. K.; Lin, S.-L.; Sauke, T. B.; Young, R. D. Orientation of Carbon Monoxide and Structure–Function Relationship in Carbonmonoxymyoglobin. *Proc. Natl. Acad. Sci. U.S.A.* **1988**, *85*, 8492–8496.
- (30) Moore, J. N.; Hansen, P. A.; Hochstrasser, R. M. Iron carbonyl bond geometries of carboxymyoglobin and carboxyhemoglobin in solution determined by picosecond time-resolved infrared-spectroscopy. *Proc. Natl. Acad. Sci. U.S.A.* **1988**, *85*, 5062.
- (31) Lim, M.; Jackson, T. A.; Anfinrud, P. A. Binding of CO to Myoglobin from a Heme Pocket Docking Site to Form Nearly linear Fe–C–O. *Science* **1995**, *269*, 962–966.
- (32) Park, E. S.; Andrews, S. S.; Hu, R. B.; Boxer, S. G. Vibrational Stark Spectroscopy in Proteins: a Probe and Calibration for Electrostatic Fields. *J. Phys. Chem. B* **1999**, *103*, 9813–9817.
- (33) Spiro, T. G.; Kozlowski, P. M. Discordant Results on FeCO Deformability in Heme Proteins Reconciled by Density Functional Theory. *J. Am. Chem. Soc.* **1998**, *120*, 4524–4525.
- (34) Lopez, M. A.; Kollman, P. A. Application of molecular-dynamics and free-energy perturbation-methods to metalloporphyrin-ligand systems. 2. CO and dioxygen binding to myoglobin. *Protein Sci.* **1993**, *2*, 1975.
- (35) Hu, S.; Vogel, K. M.; Spiro, T. G. Deformability of Heme Protein CO Adducts: FT-IR Assignment of the FeCO Bending Mode. *J. Am. Chem. Soc.* **1994**, *116*, 11187–11188.
- (36) Ghosh, A.; Bocian, D. F. Carbonyl Tilting and Bending Potential Energy Surface of Carbon Monoxymyoglobins. *J. Phys. Chem.* **1996**, *100*, 6363–6367.
- (37) Case, D. A.; Karplus, M. Stereochemistry of carbon-monoxide binding to myoglobin and hemoglobin. *J. Mol. Biol.* **1978**, *123*, 697.
- (38) Collman, J. P.; Brauman, J. I.; Iverson, B. L.; Swessler, J. L.; Morris, R. M.; Gibson, Q. H. Stereochemistry of Carbon-Monoxide Binding to Myoglobin and Hemoglobin. *J. Am. Chem. Soc.* **1993**, *105*, 3052.
- (39) (a) Pauling, L. Nature of the Iron–Oxygen Bond in Oxyhaemoglobin. *Nature* **1964**, *203*, 182–183. (b) Phillips, S. E. V.; Schoenborn, B. P. Neutron-Diffraction reveals oxygen-histidine hydrogen-bond in oxymyoglobin. *Nature* **1981**, *292*, 81. (c) Lukin, J. A.; Simplaceanu, V.; Zou, M.; Ho, N. T.; Ho, C. NMR reveals hydrogen bonds between oxygen and distal histidines in oxyhemoglobin. *Proc. Natl. Acad. Sci. U.S.A.* **2000**, *97*, 10354. (d) Unno, M.; Christian, J. F.; Olson, J. S.; Sage, J. T.; Champion, P. M. Evidence for Hydrogen Bonding Effects in the Iron Ligand Vibrations of Carbonmonoxy Myoglobin. *J. Am. Chem. Soc.* **1998**, *120*, 2670–2671.
- (40) Phillips, G. N.; Teodoro, M. L.; Li, T.; Smith, B.; Olson, J. S. Bound CO Is a Molecular Probe of Electrostatic Potential in the Distal Pocket of Myoglobin. *J. Phys. Chem.* **1999**, *103*, 8817.
- (41) Sigfridsson, E.; Ryde, U. On the Significance of Hydrogen Bonds for the Discrimination Between CO and O₂ by Myoglobin. *J. Biol. Inorg. Chem.* **1999**, *4*, 99–110.
- (42) Cornell, W. D.; Cieplak, P.; Bayly, C. I.; Merz, K. M., Jr.; Ferguson, D. M.; Spellmeyer, D. C.; Fox, T.; Caldwell, J. W.; Kollman, P. A. A 2nd generation force-field for the simulation of proteins, nucleic-acids, and organic-molecules. *J. Am. Chem. Soc.* **1995**, *117*, 5179.
- (43) La Mar, G. N.; Chatfield, M. J.; Peyton, D. H.; de Ropp, J. S.; Smith, W. S.; Dirshnamoorthi, R.; Satterlee, J. D.; Erman, J. E. Solvent isotope effects on NMR spectral parameters in high-spin ferric hemoproteins—an indirect probe for distal hydrogen-bonding. *Biochim. Biophys. Acta* **1988**, *956*, 267.
- (44) Miller, L. M.; Pedraza, A. J.; Chance, M. R. Identification of Conformational Substrates Involved in Nitric Oxide Binding to Ferric and Ferrous Myoglobin through Difference Fourier Transform Infrared Spectroscopy (FTIR). *Biochemistry* **1997**, *36*, 12199–12207.
- (45) Teng, T.-Y.; Srajer, V.; Moffat, K. Photolysis-induced structural-changes in single-crystals of carbonmonoxy myoglobin at 40K. *Nat. Struct. Biol.* **1994**, *1*, 701.
- (46) Schlichting, I.; Berendzen, J.; Phillips G. N., Jr.; Sweet, R. M. Crystal-structure of photolyzed carbonmonoxy-myoglobin. *Nature* **1994**, *371*, 808.
- (47) Carver, T. E.; Rohlfs, R. J.; Olson, J. S.; Gibson, Q. H.; Blackmore, R. S.; Springer, B. A.; Sliagar, S. G. Analysis of the kinetic barriers for ligand-binding to sperm whale myoglobin using site-directed mutagenesis and laser photolysis techniques. *J. Biol. Chem.* **1990**, *265*, 20007.
- (48) Olson, J. S.; Phillips, G. N., Jr. Kinetic pathways and barriers for ligand binding to myoglobin. *J. Biol. Chem.* **1996**, *271*, 17593.
- (49) Hu, X.; Rodgers, K. R.; Mukherji, I.; Spiro, T. G. New Light on Allostery: Dynamic Resonance Raman Spectroscopy of Hemoglobin Kempsey. *Biochemistry* **1999**, *38*, 3462.

AR000108J